

Pacemaking by HCN Channels Requires Interaction with Phosphoinositides

Gerd Zolles,¹ Nikolaj Klöcker,¹ Daniela Wenzel,²
Jutta Weisser-Thomas,² Bernd K. Fleischmann,²
Jochen Roeper,^{3,*} and Bernd Fakler^{1,*}

¹Institute of Physiology
University of Freiburg
Hermann-Herder-Strasse 7
79104 Freiburg
Germany

²Institute of Physiology
Life & Brain Center
University of Bonn
Sigmund-Freud-Strasse 25
53105 Bonn
Germany

³Institute of Physiology
Div. of Neurophysiology
University of Marburg
Deutschhausstrasse 1-2
35037 Marburg
Germany

Summary

Hyperpolarization-activated, cyclic-nucleotide-gated (HCN) channels mediate the depolarizing cation current (termed I_h or I_f) that initiates spontaneous rhythmic activity in heart and brain. This function critically depends on the reliable opening of HCN channels in the subthreshold voltage-range. Here we show that activation of HCN channels at physiologically relevant voltages requires interaction with phosphoinositides such as phosphatidylinositol-4,5-bisphosphate (PIP₂). PIP₂ acts as a ligand that allosterically opens HCN channels by shifting voltage-dependent channel activation ~20 mV toward depolarized potentials. Allosteric gating by PIP₂ occurs in all HCN subtypes and is independent of the action of cyclic nucleotides. In CNS neurons and cardiomyocytes, enzymatic degradation of phospholipids results in reduced channel activation and slowing of the spontaneous firing rate. These results demonstrate that gating by phospholipids is essential for the pacemaking activity of HCN channels in cardiac and neuronal rhythmogenesis.

Introduction

Hyperpolarization-activated, cyclic-nucleotide-gated (HCN) ion channels are widely expressed in the mammalian heart and brain, where they give rise to the slowly activating cationic current known as I_h , I_q , or I_f (Brown et al., 1979; Halliwell and Adams, 1982). Molecularly, mammalian HCN channels are assembled as homo- or heterotetramers from protein subunits encoded by the four different genes HCN1-4 (Ludwig et al., 1998;

Santoro et al., 1998). Upon heterologous expression, all HCN isoforms reproduce the functional hallmarks of their native counterparts (for review see Baruscotti et al., 2005; Kaupp and Seifert, 2001; Robinson and Siegelbaum, 2003). They open in response to membrane hyperpolarization and close upon depolarization, their activation and deactivation kinetics are slow (time constants in the range of hundreds of milliseconds to seconds), they are permeable to both Na⁺ and K⁺ ions, and their voltage-dependent gating is modulated by cAMP. Binding of cAMP to a C-terminal cyclic-nucleotide-binding domain (CNBD) shifts voltage-dependent activation of HCN channels to more depolarized potentials, thereby enhancing channel opening (DiFrancesco and Tortora, 1991; Wainger et al., 2001).

In the cellular context, HCN channels were found to be responsible for a variety of physiological functions ascribed to I_h . These are control of pacemaker activity in both heart and brain (DiFrancesco, 1993; Pape and McCormick, 1989), determination of the resting membrane potential (Williams and Stuart, 2000), and control of membrane resistance and synaptic integration in dendrites (Magee, 1999) as well as primary sensory transduction (Stevens et al., 2001).

A prerequisite for any of these functions is reliable activity of HCN channels in the subthreshold voltage range (usually between –50 mV and –80 mV), which requires “appropriate localization” of the channels’ steady-state activation curve on the voltage axis (Frere et al., 2004). This localization is dynamic, and the intracellular level of cAMP is thought to be the key mechanism for the dynamic control of voltage-dependent gating of HCN channels (DiFrancesco and Tortora, 1991). There is, however, strong experimental evidence for an additional regulatory factor that is independent of cyclic nucleotides and appears to be effective in all HCN subtypes (Chen et al., 2001; DiFrancesco et al., 1986; DiFrancesco and Mangoni, 1994). Thus, currents through native and heterologously expressed HCN channels display pronounced “run-down” in excised patches or during prolonged whole-cell recordings that results from an extensive 30–50 mV hyperpolarizing shift of the steady-state activation (Chen et al., 2001; DiFrancesco et al., 1986). Effects on the basal level of cAMP may only account for up to 15–20 mV of this shift (Chen et al., 2001). In addition, the potential required for half-maximal activation ($V_{1/2}$) of native HCN channels exhibits considerable variation among cell types (for review see Baruscotti et al., 2005; Santoro and Tibbs, 1999), or, quite explicitly in the heart, among cells of distinct regional distribution or at different developmental stages (Boyett et al., 2000; Cerbai et al., 1999; Robinson et al., 1997). Most strikingly, a 20 mV difference in $V_{1/2}$ was reported between HCN2 channels overexpressed (by viral transfection) in newborn and adult ventricular myocytes at saturating cAMP (Qu et al., 2001).

The molecular factor behind this “context dependence” (Baruscotti et al., 2005) as well as behind the run-down of HCN channels in excised patches and whole-cell recordings has remained elusive.

*Correspondence: roeper@mail.uni-marburg.de (J.R.), bernd.fakler@physiologie.uni-freiburg.de (B.F.)

Here we show that the gating of native and heterologously expressed HCN channels may be controlled by membrane phospholipids such as PIP₂. These phosphoinositides operate as allosteric ligands that shift the voltage-dependent activation of HCN channels toward depolarized potentials and thus enable robust channel activation in the voltage range relevant for the physiological role of I_h channels.

Results

Gating of HCN Channels in Dopaminergic Midbrain Neurons Is Altered by Wortmannin

HCN channels in adult dopaminergic (DA) midbrain neurons of the substantia nigra (SN; [Neuhoff et al., 2002](#)) were investigated with the perforated-patch technique in voltage- and current-clamp configuration under control conditions and after a 30 min preincubation of the brain slices with wortmannin (10 μM), an inhibitor of the type-III PI 4-kinase at micromolar concentrations ([Vanhaesebroeck et al., 2001](#); [Balla and Balla, 2006](#)). As illustrated in [Figures 1A](#) and [1B](#) (left panel), HCN channels of DA SN neurons were activated under either condition upon hyperpolarizing voltage steps. However, HCN channels in neurons pretreated with wortmannin required more hyperpolarizing voltage commands for equivalent activation compared to channels recorded under control conditions. When quantified in steady-state activation curves (see [Experimental Procedures](#)), wortmannin treatment led to a left-shift of channel activation by >10 mV, with voltages for half-maximal activation ($V_{1/2}$) of -65.4 mV and -77.6 mV determined with Boltzmann fits to the mean steady-state activation of control and wortmannin-treated HCN channels, respectively ([Figure 1C](#)). The steepness of the activation curve (slope factor) reflecting the voltage dependence of channel activation was not affected by the PI-kinase inhibitor ([Figure 1C](#); values of 7.9 mV and 7.8 mV for wortmannin-treated neurons and controls, respectively). In line with the left-shifted activation of HCN channels, the voltage response of wortmannin-treated DA SN neurons to injection of hyperpolarizing current (-50 pA, -75 pA) was markedly different from controls. Thus, the prominent voltage-sag reflecting activation of HCN channels was markedly diminished and slowed in wortmannin-treated cells, the rebound delay was prolonged, and the following spiking activity was reduced ([Figures 1A](#) and [1B](#), right panel).

The wortmannin-induced modulation of HCN gating was further investigated in perforated-patch current-clamp recordings monitoring the spontaneous firing of DA SN neurons. As illustrated in [Figures 2A](#) and [2B](#), a 20 min application of wortmannin led to a marked decrease of the spiking frequency in all neurons tested, which was not reversed by 8-bromo-cAMP (8-Br-cAMP; 100 μM) added to the bath solution in a concentration saturating for activation of HCN channels ([Figures 2A](#) and [2B](#)). Moreover, no significant effect of wortmannin was observed when HCN channels were blocked by the HCN channel blocker ZD7288 (10 μM; [Figure S2](#) in the [Supplemental Data](#) available online).

Comparison of interspike intervals obtained under control conditions and those recorded during application of wortmannin or ZD7288 (30 μM) showed that wort-

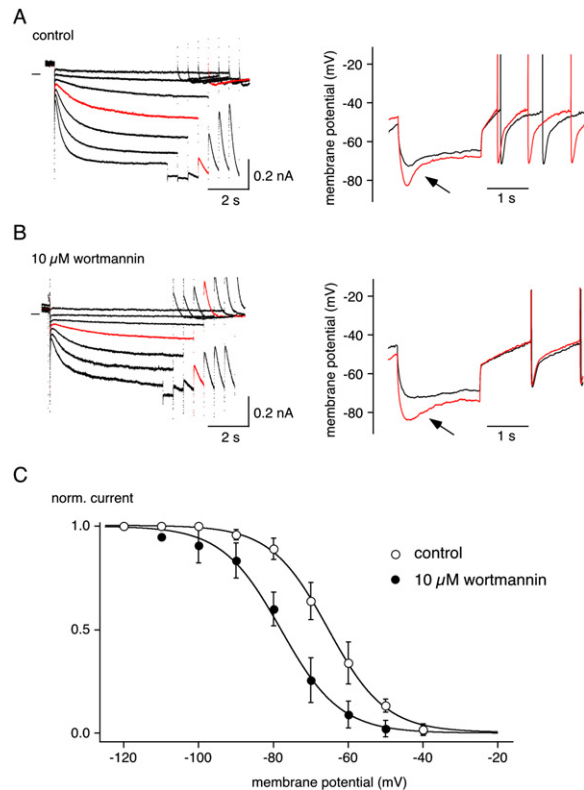


Figure 1. Modulation of HCN Gating in Dopaminergic Midbrain Neurons by Wortmannin

(A and B) (Left panels) Amphotericin perforated-patch whole-cell voltage-clamp recordings of HCN currents elicited by voltage steps of increasing amplitude (to potentials between -50 mV and -110 mV) and decreasing duration (from 8.5 s to 5.5 s) from a holding potential of -40 mV, followed by a 500 ms voltage step to -120 mV. Traces in red are current responses to voltage steps to -80 mV. (Right panels) Perforated-patch whole-cell current-clamp recordings of the membrane potential in response to 2 s current injections of -50 pA and -75 pA. Traces in red are voltage responses to -75 pA current injections. Note the reduced and slowed HCN-induced voltage sag and the prolonged spike delay after wortmannin treatment compared to control (sag amplitudes of wortmannin-treated cells and controls were 3.6 mV and 8.4 mV [for the -50 pA current injection] and 10.7 mV and 14.8 mV [for the -75 pA current injection], respectively).

(C) Steady-state activation curves of HCN channels in DA SN neurons recorded in the perforated-patch configuration in controls and after wortmannin treatment. Data points are mean ± SEM of seven experiments; continuous lines are fit of a Boltzmann function to the data with values for $V_{1/2}$ and slope factor of -65.4 mV and 7.8 mV (controls) and -77.6 mV and 7.9 mV (wortmannin), respectively. Note the shift to negative membrane potentials induced by wortmannin treatment.

wortmannin decreased the slope of the “pacemaker” depolarization without changing the threshold of firing ([Figure 2C](#)).

Together, these results indicated that the voltage-dependent gating of HCN channels is modulated by the PI 4-kinase inhibitor wortmannin and that this modulation is independent of cyclic nucleotides.

“Wash-Out” Effect on HCN Gating Is Reversed by Membrane Phospholipids

Cyclic-nucleotide-independent modulation of HCN channel gating was further observed with HCN2 mutant

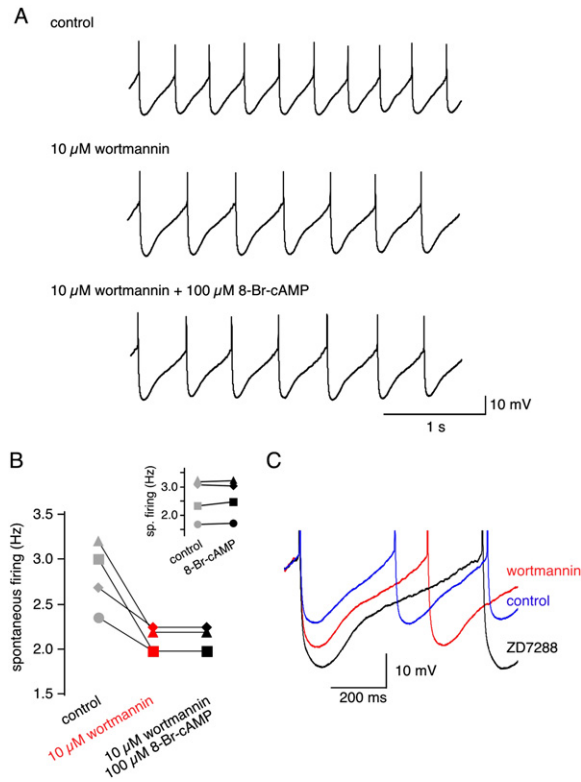


Figure 2. Effect of Wortmannin-Mediated Modulation of HCN on the Spontaneous Firing in Dopaminergic Midbrain Neurons

(A) Gramicidin perforated-patch whole-cell current-clamp recordings of spontaneous firing of a DA SN neuron under control conditions and after bath application of 10 μM wortmannin and 100 μM 8-Br-cAMP. Note that the wortmannin-induced reduction of the firing rate is not altered by the additional application of 8-Br-cAMP. (B) Mean firing rates of four spontaneously active DA SN neurons under control conditions and after application of wortmannin and 8-Br-cAMP (reduction of firing rate is significant with a p value of 0.01, paired Student's t test). (Inset) Spontaneous firing rates of another four DA SN neurons before and after application of 8-Br-cAMP (firing rates were not significantly different, $p > 0.05$, paired Student's t test). (C) Interspike intervals of spontaneously active DA SN neurons under control conditions and after wortmannin application or after complete inhibition of HCN currents by 30 μM ZD7288.

channels that lack cAMP binding [HCN2(R591E) (Chen et al., 2001) and HCN2(ΔCNBD) (Wainger et al., 2001)]. Following patch excision from *Xenopus* oocytes, currents mediated by HCN2(R591E) channels and activated by a hyperpolarizing voltage step to -120 mV successively decreased in amplitude (to $\sim 20\%$ of the cell-attached value), while their rising phase was successively slowed (~ 3 -fold increase in activation time constant; Figure 3A, inset). The changes in both amplitude and activation time course resulted from a shift of the activation curve to more hyperpolarized potentials, which, after a 5 min perfusion of the inside-out (i-o) patches, exhibited values of ~ 20 mV ($V_{1/2}$ of -120.3 mV; Figure 3B). Similarly, the steady-state activation curve of HCN2 wild-type channels was largely shifted to the left upon perfusion of i-o patches. As shown in Figure 3B, the respective shift at steady-state wash-out was ~ 40 mV ($V_{1/2}$ of -120.1 mV; Figure 3B), with half of this value

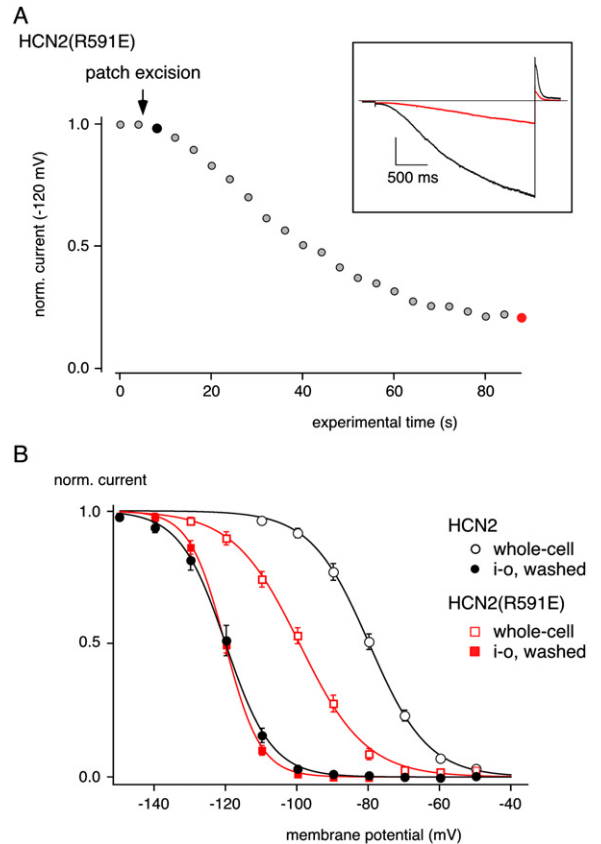


Figure 3. Shift in Voltage-Dependent Gating of HCN Channels by Perfusion of Excised i-o Patches

(A) Currents mediated by cAMP-insensitive HCN2(R591E) channels decrease in amplitude following patch excision. Currents were measured in response to successive 2.5 s voltage steps to -120 mV (from a holding potential of 0 mV, tail potential 50 mV) and normalized to the cell-attached amplitude. (Inset) Current traces recorded at the indicated time points; values for $\tau_{\text{activation}}$ were 1.25 s (black trace), 3.38 s (red trace). Current scale is 1 nA, timescale as indicated, horizontal line is zero current. (B) Steady-state activation curves of HCN2 wt and HCN2(R591E) mutant channels determined in whole oocytes and inside-out patches after a 5 min perfusion. Data points are mean (\pm SEM) of ten (patches) and seven (whole-cell) experiments, respectively. Lines are fit of a Boltzmann function to the data with values for $V_{1/2}$ and slope factor of -79.8 mV and 8.1 mV (HCN2 wt, whole cell) and -120.1 mV and 6.5 mV (HCN2 wt, i-o patch), -99.4 mV and 9.2 mV [HCN2(R591E), whole cell], and -120.3 mV and 5.1 mV [HCN2(R591E), i-o patch].

($\Delta V_{1/2}$ of 19.2 ± 2.3 mV, $n = 6$) being due to the wash-out of cAMP. The remaining cAMP-independent shift in HCN2 wt as well as the shift observed with the cAMP-insensitive mutant HCN2(R591E) has been attributed to a yet unknown modulatory mechanism (Baruscotti et al., 2005; Santoro and Tibbs, 1999).

Prompted by the gating effect of wortmannin on native HCN channels and the known enzymatic degradation of phospholipids in perfused i-o patches (Baukrowitz et al., 1998; Huang et al., 1998; Oliver et al., 2004), phosphatidylinositol-4,5-bisphosphate (PIP₂) under saturating conditions (Figure S1) was probed for its effect on HCN2 channels. As illustrated in Figure 4, the phospholipid added as suspension (see Experimental Procedures) induced an ~ 20 mV shift of the activation

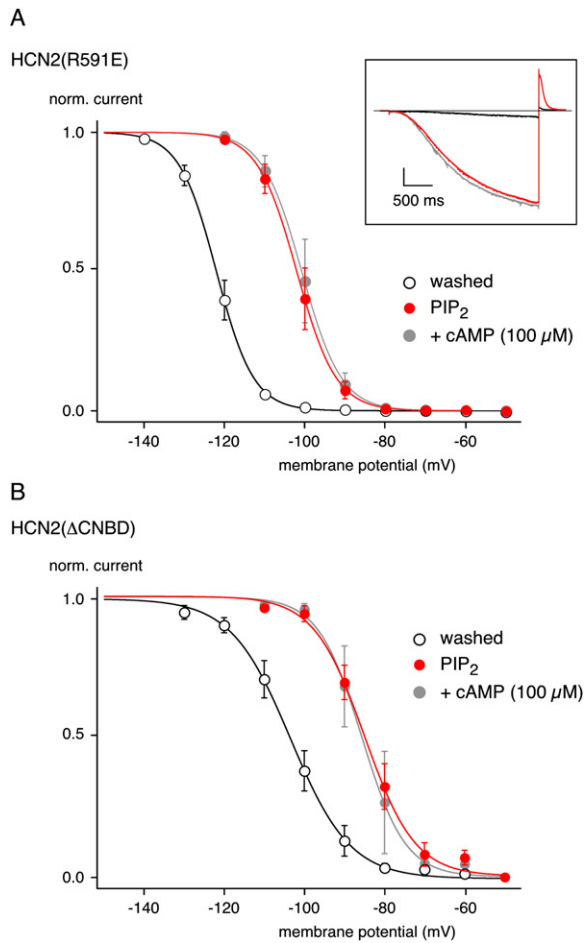


Figure 4. Reverse Shift in Voltage-Dependent Gating of HCN Channels by PIP₂

(A) Steady-state activation curves of HCN2(R591E) mutant channels determined before (washed) and after a 5 s application of PIP₂ (10 μM; red) and during subsequent application of cAMP (100 μM; gray). Data points are mean (±SEM) of four patches. Lines are fit of a Boltzmann function to the data with values for V_{1/2} and slope factor of -122.0 mV and 4.6 mV (washed), -102.1 mV and 4.9 mV (PIP₂), -100.8 mV and 4.9 mV (+cAMP). (Inset) Representative current traces recorded in response to a step potential of -110 mV (from a holding potential of 0 mV, tail potential 50 mV), values for τ_{activation} were 1.91 s (washed), 0.95 s (PIP₂), and 0.86 s (+cAMP). Current scale is 1 nA, timescale as indicated, horizontal line is zero current.

(B) Steady-state activation curves as in (A) for HCN2(ΔCNBD) mutant channels. Data points are mean (±SEM) of four patches. Lines are fit of a Boltzmann function to the data with values for V_{1/2} and slope factor of -103.4 mV and 7.4 mV (washed), -85.7 mV and 5.8 mV (PIP₂), -84.9 mV and 6.3 mV (+cAMP).

curve toward depolarized potentials when applied to HCN2(R591E) ($\Delta V_{1/2}$ of 20.1 ± 3.2 mV, $n = 4$) or HCN2(ΔCNBD) ($\Delta V_{1/2}$ of 19.1 ± 1.5 mV, $n = 4$) channels after steady-state wash-out. Viewed as response to a voltage step to -110 mV, this right-shift in channel activation translated into currents with markedly increased amplitude and accelerated rising phase (Figure 4A, inset).

Very similar results were obtained with PIP₂ applied to extensively perfused HCN2 wild-type channels. Thus, the steady-state activation curve was shifted to the right by 18.0 ± 0.8 mV ($\Delta V_{1/2}$; $n = 10$) at constant slope factor

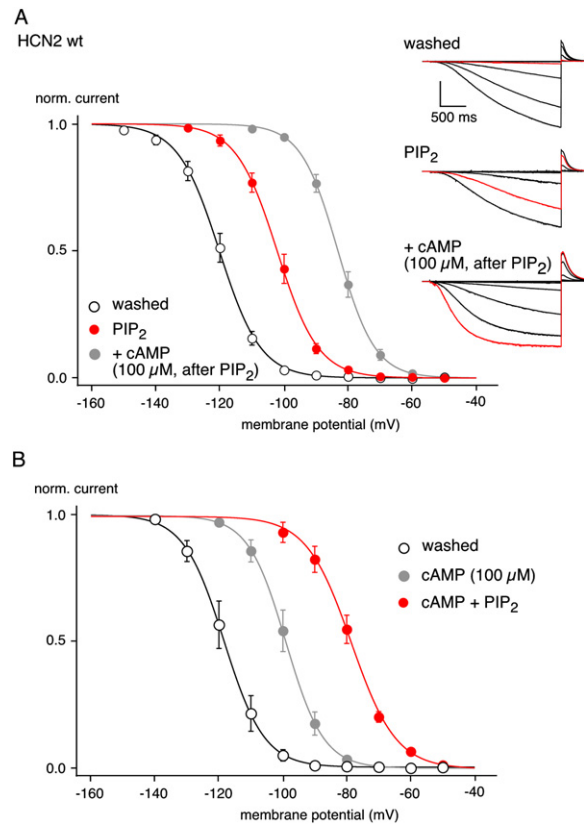


Figure 5. PIP₂-Mediated Shift in HCN Gating Is Not Affected by cAMP

(A) Steady-state activation curves of HCN2 channels determined before (washed) and after a 5 s application of PIP₂ (10 μM; red) and during subsequent application of cAMP (100 μM; gray). Data points are mean (±SEM) of ten patches. Lines are fit of a Boltzmann function to the data with values for V_{1/2} and slope factor of -120.1 mV and 6.4 mV (washed), -102.1 mV and 6.4 mV (PIP₂), and -83.1 mV and 5.9 mV (+cAMP after PIP₂). (Inset) Representative current traces recorded in response to voltage steps to potentials between -50 mV and -140 mV (washed), -120 mV (PIP₂) or -110 mV (+cAMP after PIP₂) in 10 mV increments (holding potential was 0 mV, tail potential 50 mV). Traces in red are responses to a step potential of -110 mV; current scale is 1 nA, timescale as indicated.

(B) Steady-state activation curves as in (A) determined before (washed) and during application of cAMP prior to (100 μM; gray) and after a 5 s application of PIP₂ (10 μM; red). Data points are mean (±SEM) of six patches. Lines are fit of a Boltzmann function to the data with values for V_{1/2} and slope factor of -118.4 mV and 6.3 mV (washed), -99.1 mV and 5.9 mV (cAMP), and -78.6 mV and 6.9 mV (cAMP+PIP₂).

and the time course of channel activation (at a given test potential) was accelerated over the entire voltage range tested (Figure 5A). The channel conductance remained unaffected (mean ± SD of the rel. conductance after PIP₂ application was 0.99 ± 0.12 of that obtained after steady-state wash-out, $n = 8$). Different from the HCN2(R591E) and HCN2(ΔCNBD) mutants, activation of wild-type channels was further shifted to the right by 19.1 ± 2.1 mV ($\Delta V_{1/2}$; $n = 10$) upon subsequent application of 100 μM cAMP (Figure 5A). The resulting activation curve exhibited a V_{1/2} of -83.1 ± 3.2 mV ($n = 10$), closely matching the value determined in voltage-clamp recordings from whole oocytes (V_{1/2} = -80.1 ± 2.1 mV, $n = 7$; Figure 3B). The V_{1/2} shifts obtained with both

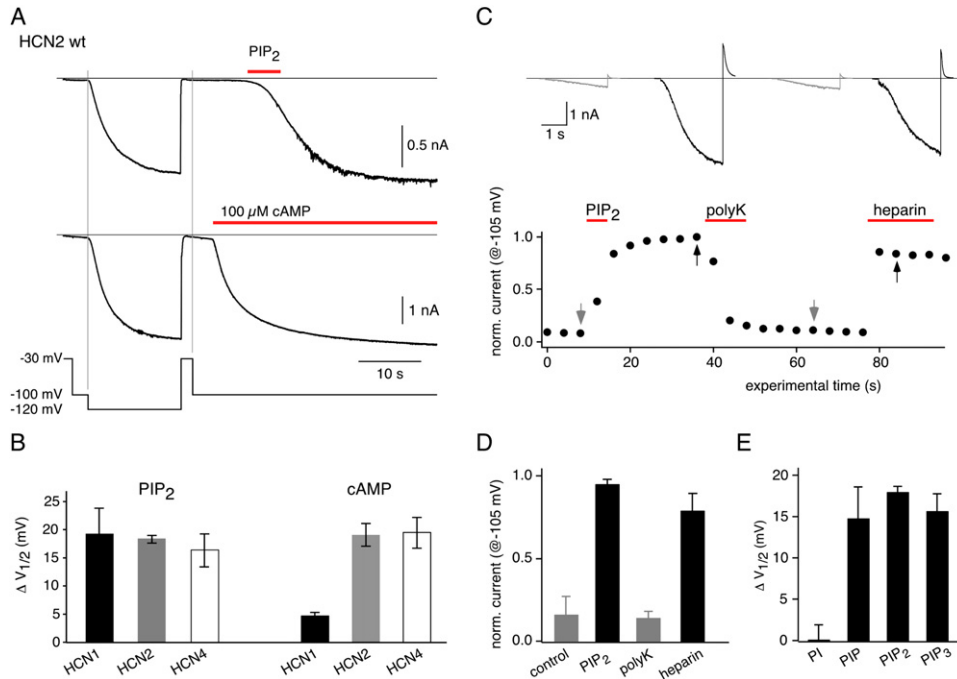


Figure 6. HCN Gating by Phospholipids Is Mediated by the Negatively Charged Headgroups of Membrane-Inserted Phosphoinositides
(A) Current recordings in response to the indicated voltage protocol and the application of PIP₂ (10 μM; upper panel) or cAMP (100 μM; lower panel); current and time scaling as indicated. Note that activation by either ligand equalled that of a 20 mV hyperpolarization.
(B) Summary of the shift in activation curve induced by PIP₂ and cAMP in the HCN channel subtypes indicated. Data are mean (±SD) of ten (HCN1, HCN2) and four (HCN4) patches, respectively.
(C) Shift in voltage-dependent activation of HCN2 by PIP₂ (10 μM, 5 s) was removed by polyK (25 μg/ml). Subsequent application of heparin (100 μg/μl) restored the effect of PIP₂. Currents were recorded in response to 2.5 s voltage steps from 0 mV to −105 mV followed by 0.5 s step to 50 mV. (Insets) Traces recorded at the time points indicated by arrows. Traces recorded after PIP₂ and with heparin are in black; traces recorded prior to PIP₂ and after polyK are in gray.
(D) Summary of the effects of PIP₂, polyK, and heparin; data are mean ± SD of six patches.
(E) Phosphatidylinositol-4-phosphate (PIP), PIP₂, and phosphatidylinositol-3,4,5-triphosphate (PIP₃) (10 μM, 5 s; each) shifted voltage-dependent activation of HCN2 channels, whereas PI (20 μM, 5 s) failed. Data are mean ± SD of five (PI), four (PIP), ten (PIP₂) and six (PIP₃) experiments.

PIP₂ and saturating cAMP were independent of the order of application (Figure 5B), with $\Delta V_{1/2}$ values of 18.4 ± 2.6 mV (PIP₂ in the presence of cAMP; $n = 6$) and 19.2 ± 2.3 mV (cAMP prior to PIP₂; $n = 6$). In addition, the affinity of HCN2 channels for cAMP was not affected by the phospholipid (data not shown).

Together, these results indicated that PIP₂ determines the voltage range of HCN2 channel gating independently of cyclic nucleotides and that the combined effects of PIP₂ and cAMP were able to restore channel activation in excised patches to its appearance in intact cells.

Activation of HCN Channels by Membrane Phospholipids

The observed 20 mV shift in steady-state activation implies that PIP₂ and cAMP should induce robust opening of HCN2 channels when applied at appropriately negative membrane potentials. This was tested in experiments that used motor-driven fast application of either activating molecule to washed-out HCN2 channels at a constant membrane potential. As shown in Figure 6A, PIP₂ and cAMP effectively activated HCN2 channels at a test potential of −100 mV, where no or very little channel activity was observed prior to application. The activating potency of both molecules was similar and equalled that of a 20 mV hyperpolarization, as reflected

by the current response to a voltage step from −100 mV to −120 mV preceding the application of PIP₂ or cAMP (Figure 6A).

Thus, both PIP₂ and cAMP may be regarded as ligands that allosterically activate HCN2 channels, supposedly though by distinct mechanisms. This was further investigated by probing both ligands for effects on other HCN subtypes as well as by further characterizing the mode of action of the PIP₂ molecule. As illustrated in Figure 6B, the activation properties of PIP₂ and cAMP were distinct among HCN subtypes. Thus, in HCN4, both molecules shifted the activation curve by >15 mV, while in HCN1 channels the $V_{1/2}$ shift induced by the phospholipid largely exceeded that of the cyclic nucleotide (Figure 6B). Moreover, channel activation by cAMP required its continuous presence and was rapidly reversed upon wash-out (Figure 6A), while channel activation by PIP₂ occurred after brief application (Figure 6A) and persisted despite extensive perfusion with PIP₂-free solution for as long as the excised patches remained stable. The effect of PIP₂, however, was abolished by poly-lysine (polyK, 25 μg/ml), a poly-cation that tightly binds to the negatively charged head moiety of PIP₂, and it was almost fully restored upon subsequent application of heparin, a poly-anion known to remove polyK from patches (Oliver et al., 2004; Figures 6C and

6D). The prolonged duration of the PIP₂ effect and its sensitivity to charge-shielding suggested that phosphoinositide-mediated activation of HCN channels requires insertion of the phospholipid into the plasma membrane and a negative moiety at its headgroup, similar to what is known for PIP₂-mediated gating modulation of Kir and Kv channels (Huang et al., 1998; Oliver et al., 2004; Rohacs et al., 2003; Shyng and Nichols, 1998). The contribution of the negatively charged headgroups was further investigated using phosphoinositides with a variable number of phosphate groups at the inositol ring. As summarized in Figure 6E, all phospholipids bearing a negatively charged headgroup were about equally effective, while phosphatidylinositol (PI) with its fully dephosphorylated inositol ring failed to shift the activation curve of HCN channels.

Together, these results indicated that both PIP₂ and cAMP operate as ligands that allosterically activate HCN channels and that channel activation by PIP₂ is mediated by membrane-inserted phosphoinositides through electrostatic interactions.

Alteration of HCN Gating by Enzymatic Modulation of Phospholipids

Next, the modulation of HCN channel gating induced by interference with enzymatic activities required for maintenance of phospholipids was probed in *Xenopus* oocytes and cultured cells. First, the membrane-associated lipid phosphatases of oocytes that are known to be very active in excised patches (Huang et al., 1998) were inhibited by addition of fluoride (5 mM), vanadate (0.1 mM), and pyrophosphate (10 mM) to the perfusion solution (FVPP solution, see Experimental Procedures). As shown in Figure 7A, this largely slowed the decay of HCN2-mediated currents (n = 6) observed under control conditions (cAMP-containing intracellular solution). When approximated with monoexponentials, the respective time constants for the current decay (mean ± SD) were 35.0 ± 15.8 s (n = 6) in control conditions and 286.4 ± 105.2 s (n = 5) after addition of FVPP.

A second set of experiments decreased the amount of PIP₂ in the plasma membrane either by inhibition of the PI 4-kinase (wortmannin, 10 μM) or by coexpression of the membrane-targeted inositol 5-phosphatase domain of synaptojanin 1, a highly active PIP₂ phosphatase (Milosevic et al., 2005). Thus, the steady-state activation curve of HCN2 channels expressed in CHO cells and recorded in whole-cell configuration was left-shifted by ~10 mV (Figure 7B, left panel) after wortmannin-treatment, similar to the observation on native HCN channels in DA SN neurons (Figure 1A). The slope factor of the activation curve was not affected by wortmannin (Figure 7B, left panel). Similar results for wortmannin-induced changes in the activation curve were obtained with HCN1 channels expressed in CHO cells (ΔV_{1/2} induced by wortmannin treatment was 9.1 mV; data not shown). Coexpression of synaptojanin in *Xenopus* oocytes resulted in an ~10 mV left-shift of the steady-state activation curve of HCN2 channels at constant slope factor (Figure 7B, right panel).

These results confirm the effects obtained with PIP₂ application onto excised patches and suggest that phosphoinositides may be regulators of HCN channel gating under cellular conditions.

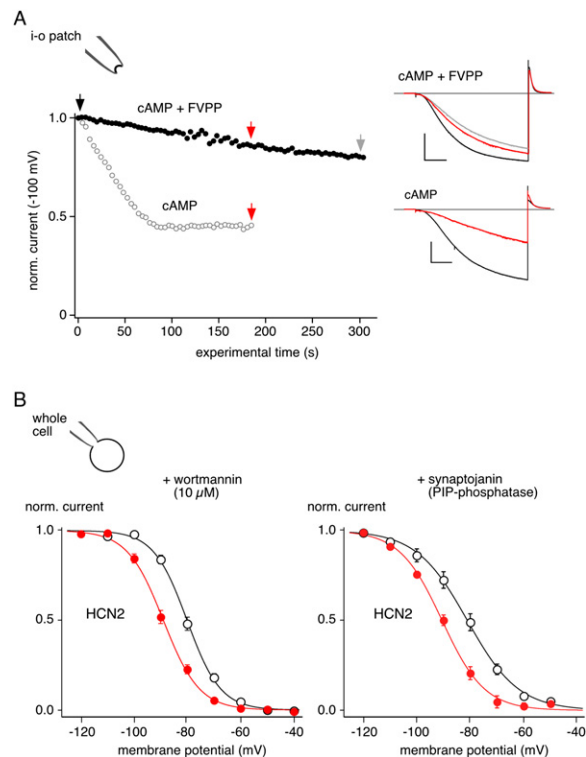


Figure 7. Modulation of HCN Gating by Enzymatic Alteration of Membrane Phosphoinositides

(A) Addition of FVPP to the internal solution slows the decrease of HCN2-mediated currents induced by patch excision from *Xenopus* oocytes. Data points are maximal currents (normalized to the amplitude recorded in cell-attached configuration right before patch excision) recorded in response to successive 2.5 s voltage steps to -100 mV in the absence (open gray) or presence of FVPP (filled black) in the cAMP (100 μM) containing perfusion solution. (Insets) Current traces recorded at the time points indicated by arrows; scale bars are 1 nA and 0.5 s.

(B) (Left panel) Steady-state activation curves of HCN2 channels expressed in CHO cells under control conditions (open black) or after preincubation with wortmannin (10 μM, 30 min; filled red). Data points are mean ± SEM of seven cells. Lines are fit of a Boltzmann function to the data with values for V_{1/2} and slope factor of -79.9 mV and 6.3 mV (control), -89.0 mV and 6.7 mV (wortmannin). (Right panel) Steady-state activation curves of HCN2 channels expressed alone (open black) or together with the PIP₂ phosphatase synaptojanin (filled red) in *Xenopus* oocytes. Activation curves were determined in recordings from whole oocytes; data points are mean ± SEM of six (coexpression of synaptojanin) and eight (control) oocytes. Lines are fit of a Boltzmann function to the data with values for V_{1/2} and slope factor of -81.0 mV and 9.5 mV (control), -90.5 mV and 7.9 mV (synaptojanin).

Phospholipid Regulation of HCN Gating in Cardiomyocytes

Regulation by phosphoinositides may be expected to be a general property of HCN channels and should, therefore, be cell-type and tissue independent. This was tested by probing HCN channels in cardiomyocytes for their sensitivity to modulation in membrane phospholipids. Figure 8A illustrates HCN-mediated currents recorded in an early embryonic (E9.5) cardiomyocyte in response to hyperpolarizing voltage steps immediately after establishing whole-cell configuration and after a 10 min application of wortmannin (10 μM). Similar

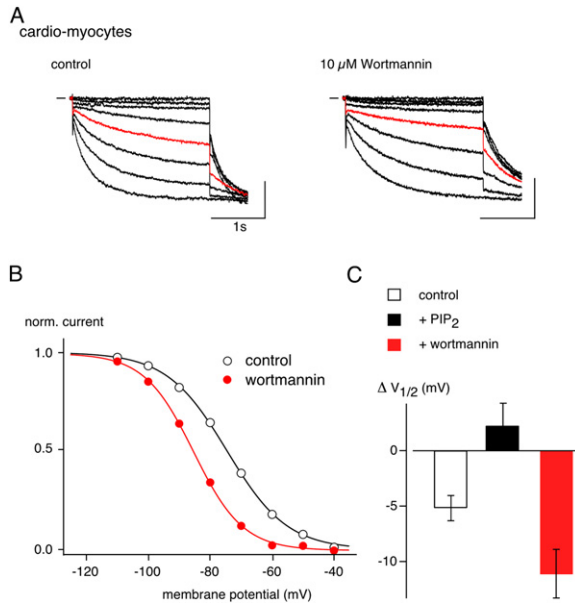


Figure 8. Phosphoinositide-Dependent Gating of HCN Channels in Embryonic Cardiomyocytes

(A) HCN-mediated currents recorded under control conditions (left panel; 100 μ M 8-Br-cAMP in the bath solution) and after a 10 min application of wortmannin (10 μ M, 100 μ M 8-Br-cAMP in the bath solution) in response to 2.5 s voltage-steps to potentials between -40 mV and -110 mV (10 mV increment, holding potential -40 mV) followed by a voltage step to -110 mV. Red traces are responses to a step potential of -80 mV; current scaling is 0.1 nA, time scaling as indicated.

(B) Steady-state activation curves obtained from representative experiments as in (A). Lines are fit of a Boltzmann function to the data with values for $V_{1/2}$ and slope factor of -74.4 mV and 9.7 mV (control), -84.9 mV and 7.9 mV (wortmannin).

(C) Summary of $V_{1/2}$ shifts obtained under the experimental conditions indicated. Data are mean \pm SEM of seven (control), four (PIP₂), and seven (wortmannin) cardiomyocytes. PIP₂ (20 μ M) was added to the whole-cell pipette, wortmannin (10 μ M) was added to the bath solution; all solutions contained 8-Br-cAMP (100 μ M).

to the observations described above in neurons and heterologous systems, steady-state activation curves of cardiac HCN channels were shifted \sim 10 mV to the left by wortmannin treatment (Figures 8B and 8C); this shift was independent of cyclic nucleotides, as saturating levels of intracellular cAMP were maintained by addition of 8-bromo-cAMP (100 μ M) to the bath solution (control). In contrast to the perforated-patch recordings from DA SN neurons (Figures 1 and 2), wash-out of the cardiomyocytes via the whole-cell pipette resulted in left-shift of the activation curve with a $\Delta V_{1/2}$ of 5.2 ± 1.2 mV (mean \pm SEM of 7 cells). This wash-out was prevented by addition of PIP₂ (20 μ M) to the pipette solution (Figure 8C).

Discussion

The central finding of this work is that activation of HCN channels in the physiological voltage range and hence its classical role in rhythmogenesis requires interaction with phosphoinositides such as PIP₂. These phospholipids produce a right-shift of the steady-state activation by \sim 20 mV and, together with cAMP, restore channel

activation in excised patches to their appearance in intact cells. The results establish PIP₂ as a novel and independent modulator of HCN channel gating and suggest that phosphoinositides may be the missing regulatory factor of I_h physiology.

Characteristics of HCN Channel Gating by Phosphoinositides

This latter suggestion arises from coincidence of the characteristics described here for PIP₂-mediated gating modulation and the hallmarks of the unknown regulatory factor thought to be responsible for "context dependence" or "run-down" of HCN-mediated currents (Baruscotti et al., 2005; Robinson and Siegelbaum, 2003). First, enzymatic degradation of phosphoinositides changes activation of HCN gating in all cell types investigated (Figures 1, 7, and 8), and application of exogenous PIP₂ reversed the channel run-down induced by extensive wash-out (Figures 3–5 and Pian et al., 2006). Second, phosphoinositide modulation of HCN gating is different from and independent of cyclic nucleotides. This is emphasized by the identical effectiveness of PIP₂ in both HCN2 wild-type (Figure 5) and the cAMP-insensitive mutants R591E and Δ CNBD (Figure 4), as well as by the observation that the PIP₂-induced shift in activation was independent of whether the phospholipid was applied before or together with saturating concentrations of cAMP (Figure 5). Independence of phosphoinositide and cyclic-nucleotide gating, however, was only observed here with the physiologically occurring long-chain fatty acid PIP₂, while water-soluble dioctanoylphosphoinositides (short-chain fatty acids) appear to be affected by cAMP (Pian et al., 2006). Third, PIP₂ proved to be equally effective in all HCN subtypes tested (HCN1, 2, 4; Figure 6B) similar to what was previously suggested for the unknown regulatory factor in native and heterologously expressed HCN channels (Chen et al., 2001).

Mechanistically, activation of HCN channels is mediated by phosphoinositides inserted into the plasma membrane (Figure 6C) and occurs through electrostatic interactions between their negatively charged head-group and the channel protein (Figures 6C–6E), similar to PIP modulation of gating in Kv (Oliver et al., 2004) and Kir channels (Baukrowitz et al., 1998; Huang et al., 1998; Shyng and Nichols, 1998). As a consequence of the lipid-protein interaction, voltage-dependent activation of HCN channels is facilitated, or, at appropriately negative membrane potentials, opening of the channel pore is initiated (Figure 6A). The PIP₂ action thus closely resembles that of cyclic nucleotides, which also trigger channel opening in a ligand-like manner (Figure 6A), although most likely by acting through different domain(s) of the HCN protein, as evidenced by the dissociation of both the cAMP and PIP₂ effect in HCN1 (Figure 6). In HCN1 channels, the cAMP-mediated shift in $V_{1/2}$ is largely reduced with respect to HCNs 2 and 4, in contrast to the phosphoinositide-mediated $\Delta V_{1/2}$ that is similar in all HCN subtypes.

Taking these characteristics into account and analogous to the mechanism underlying activation of HCN channels by cAMP (Ulens and Siegelbaum, 2003; Wainger et al., 2001; Zagotta et al., 2003), the phosphoinositide effect may result from relieving inhibition of

channel opening imposed by a protein domain different from the CNBD (Ulens and Siegelbaum, 2003; Wainger et al., 2001). Both, the inhibitory actions by the CNBD and by the “PIP domain” operate independent of each other and combine to shift the HCN2 activation curve to the left by ~40 mV when both ligands are absent. Vice versa, binding of PIP₂ and cAMP to their respective sites may cause maximal disinhibition and thus allow for efficient channel activity in the physiological subthreshold voltage range (Figures 4–6). Alternative to action via different domains, phosphoinositides and cyclic nucleotides may act through linked domains with a “coupling efficiency” beyond our detection threshold. However, both the PIP₂ interaction site on the channel protein as well as the proposed mechanism of action still awaits verification and further determination.

Physiological Significance of Gating Regulation by Phospholipids

The physiological functions of HCN channels, in particular their control of pacemaking in heart and brain, critically depend on reliable opening of the channels in a narrow subthreshold voltage window (Baruscotti et al., 2005; Frere et al., 2004; Robinson and Siegelbaum, 2003). Consequently, a 20 mV shift of the activation curve, as observed after depletion of PIP₂ from the plasma membrane (Figure 5), should profoundly impact on the I_h physiology, as shown here for the spontaneous spiking of DA SN neurons. Depletion of PIP₂ (by wortmannin-mediated inhibition of the PI 4-kinase) not only shifted steady-state activation of the HCN channels by ~10 mV (Figures 1 and 2) but also slowed down the frequency of spontaneous firing in all neurons tested (Figure 2).

Profound cAMP-independent variations in the midpoint of voltage-dependent activation are well-documented for HCN channels expressed in cardiac cells of different developmental stage or distinct regional distribution (Cerbai et al., 1999; Qu et al., 2001; Robinson et al., 1997). Based on the observed PIP₂ effects on recombinant and native HCN channels in cardiomyocytes (Figures 5 and 8), it might be interesting to investigate the developmental and localization-dependent properties for potential involvement of phosphoinositides.

Experimental Procedures

Recordings from Adult Dopaminergic Neurons in Brain Slices

250 μm coronal midbrain slices of 3-month-old male C57Bl6/J mice were sectioned after intracardial perfusion with ice-cold sucrose-ACSF (in mM): 50 sucrose, 75 NaCl, 25 NaHCO₃, 2.5 KCl, 1.25 NaH₂PO₄, 0.1 CaCl₂, 6 MgCl₂, and 2.5 glucose, oxygenated with 95% O₂, 5% CO₂. After 90 min of recovery, slices were transferred to a recording chamber and perfused continuously at 2–4 ml/min with oxygenated ACSF (2.5 mM glucose, 22.5 mM sucrose) at 36°C. Fast excitatory and inhibitory synaptic transmission was inhibited by 20 μM CNQX and 10 μM gabazine. Dopaminergic (DA) midbrain neurons in the substantia nigra (SN) were identified using accepted anatomical landmarks (SN lateral of lemniscus medialis) in combination with their typical electrophysiological properties, like spontaneous pacemaker activities and broad action potentials. Perforated-patch recordings, data acquisition, and analysis were as previously described (Neuhoff et al., 2002). For voltage-clamp recordings, amphotericin (50 mg/ml DMSO stock, final 50 μg/ml in pipette solution) was used for pore formation, resulting in low series resistances (Rs < 20 MΩ, Rs compensation at 75%, voltage errors < 5 mV). For stable long-term current-clamp recordings

of spontaneous activity, gramicidin (50 mg/ml DMSO stock, 100 μg/ml final in pipette solution) was used for pore formation.

Steady-state activation curves were determined with a tail-current protocol. Briefly, preconditioning voltage steps (from a holding potential of -40 mV) were applied to potentials between 0 mV and -120 mV for durations ranging between 9 s and 5 s, before the membrane potential was stepped to -120 mV for 500 ms to elicit HCN tail currents. Tail currents were normalized to maximum, plotted against the preconditioning potential, and fitted with a Boltzmann function: $I(\text{norm}) = 1/(1 + \exp((V - V_{1/2})/k))$. $V_{1/2}$ is voltage required for half-maximal activation; k is the slope factor.

Electrophysiology and Data Analysis of Cloned HCN Channels

Preparation and injection of cRNA into *Xenopus* oocytes and site-directed mutagenesis were done as described (Fakler et al., 1995); cell culturing and transfection of cDNAs were performed as detailed in Ludwig et al. (2001). All cDNAs were verified by sequencing; GeneBank accessions of the clones used were AJ225123.1 (HCN1), AJ225122.1 (HCN2), AJ132429.1 (HCN4). The membrane-targeted 5-inositol phosphatase domain of synaptojanin 1 was a gift of Dr. V. Haucke (Krauss et al., 2003; Milosevic et al., 2005).

Electrophysiological recordings from giant inside-out patches excised from oocytes were performed at room temperature (22°C–24°C) as described previously (Fakler et al., 1995). Briefly, currents were recorded with an EPC9 amplifier, low-pass filtered at 1 kHz, and sampled at 2 kHz; capacitive transients were compensated with the automated circuit of the EPC9. Pipettes made from thick-walled borosilicate glass had resistances of 0.3–0.6 MΩ when filled with (in mM): 120 KCl, 10 HEPES, and 1.0 CaCl₂, pH adjusted to 7.2. Intracellular solution (K_{in}) applied via a gravity-driven multi-barrel pipette was composed as follows (mM): 100 KCl, 10 K₂EGTA, 10 HEPES (pH 7.2); intracellular solution with phosphatase-inhibitors (Huang et al., 1998; Woscholski et al., 1995; FVPP-solution) contained (in mM): 55 KCl, 5 KF, 10 K₄O₇P₂, 0.1 Na₂VO₄, 10 K₂EGTA, 10 HEPES (pH 7.2). All substances were dissolved and diluted to their final concentration in intracellular solution. L-α-Phosphatidyl-D-myo-inositol-4,5-bisphosphate (PIP₂, Roche Molecular Diagnostics or Avanti Polar Lipids), L-α-Phosphatidylinositol-3,4,5-trisphosphate (PIP₃), L-α-Phosphatidylinositol-4-monophosphate (PIP) and L-α-Phosphatidylinositol (PI) were suspended in intracellular solution at a concentration of 1 mM, sonicated for 10 min in a cold water bath, aliquoted, and stored at -20°C. Samples were thawed on the day of use, sonicated for another 10 min, and diluted to their final concentration of 10 μM with intracellular solution. Two electrode-voltage-clamp recordings were obtained 2–3 days after cRNA injection. Currents were recorded with a TURBO TEC 01C amplifier (npi), low-pass filtered at 1 kHz, and sampled at 2 kHz using an ITC-16 interface and Patchmaster software (HEKA). Electrodes were filled with 3 M KCl and had resistances of 0.1–0.2 MΩ. Extracellular solution was composed as follows (mM): 100 KCl, 17.5 NaCl, 10 HEPES, and 1.8 CaCl₂ (pH 7.3).

Whole-cell patch-clamp recordings on Chinese hamster ovary (CHO) cells were done at room temperature (22°C–24°C) as previously described (Bildl et al., 2004; Oliver et al., 2001). Briefly, currents were recorded with an EPC9 amplifier, filtered at 1 kHz, and sampled at 2 kHz. Recording pipettes made from quartz glass had resistances of 1–5 MΩ when filled with (in mM): 135 KCl, 2.5 MgCl₂, 2.4 CaCl₂, 3 NaATP, 0.1 NaGTP, 5 EGTA, and 5 HEPES (pH 7.3). The extracellular solution contained (in mM): 144 NaCl, 5.8 KCl, 0.9 MgCl₂, 1.3 CaCl₂, 0.1 NaH₂PO₄, 5.6 D-glucose, and 10 HEPES (pH 7.4). Wortmannin (Sigma, Germany) was dissolved in DMSO at a stock concentration of 10 mM, stored at -20°C, and used at a final concentration of 10 μM (diluted in extracellular solution).

Steady-state activation curves were determined with a tail-current protocol. Briefly, preconditioning voltage steps (from a holding potential of 0 mV) were applied to potentials between -30 mV and -150 mV for durations ranging between 1.5 s and 5 s, before the membrane potential was stepped to 50 mV for 500 ms to elicit HCN tail currents. Currents recorded at the tail potential were normalized to maximum, plotted versus the preconditioning potential, and fitted with a Boltzmann function (see above). Curve fitting and further data analysis were done with Igor Pro 4.05A on a Macintosh G4. Data are given as mean ± SD, unless otherwise stated.

Recordings from Early Embryonic Cardiomyocytes

Murine embryonic cardiomyocytes were isolated at day E9.5 as described (Fleischmann et al., 2004) and kept on coverslips for 2 days. For electrophysiological recordings, the coverslips were placed into a recording chamber and superfused with extracellular solution containing (in mM): NaCl 140, KCl 5.4, MgCl₂ 2, CaCl₂ 1.8, HEPES 10, glucose 10 (pH 7.4).

Patch-clamp experiments in the whole-cell configuration were performed as detailed in Fleischmann et al. (2004). The following solutions were used for electrophysiological recordings (mM). External solution: NaCl 140, KCl 5.4, MgCl₂ 2, CaCl₂ 1.8, HEPES 10, glucose 10, BaCl₂ 1, 4-aminopyridine 2 (pH 7.4); internal solution: NaCl 12, HEPES 10, MgATP 2, EGTA 10, NaGTP 0.1, K-aspartate 130 (pH 7.2).

Steady-state activation curves were determined with a tail-current protocol as in Figure 8A; voltage was stepped for 2.5 s to potentials between -40 mV and -110 mV (10 mV increments) from a holding potential of -40 mV followed by a 2.5 s voltage step to either -110 mV or 15 mV (frequency 0.1 Hz) (Abi-Gerges et al., 2000). V_{1/2} and slope values were obtained from fits of a Boltzmann function to the data as described above.

8-Br-cAMP (Sigma, Germany) stored at -20°C was diluted in H₂O and used at a final concentration of 100 μM; wortmannin (Sigma, Germany) was dissolved in DMSO at a stock concentration of 10 mM, stored at -20°C, and used at a final concentration of 10 μM (diluted in extracellular solution). PIP₂ was handled as described above and used at a final concentration of 20 μM in the pipette solution. For analysis of PIP₂ experiments exclusively cells with a stable R_s < 15 MΩ were used.

Supplemental Data

The Supplemental Data for this article can be found online at <http://www.neuron.org/cgi/content/full/52/6/1027/DC1/>.

Acknowledgments

We thank Drs. J.P. Adelman and D. Oliver for insightful discussions and critical reading of the manuscript; and P. Sasse for help with recordings from cardiomyocytes. This work was supported by the Graduate School GRK 843 and by the grant KL 1168/6 of the Deutsche Forschungsgemeinschaft to N.K.

Received: September 26, 2006

Revised: November 8, 2006

Accepted: December 5, 2006

Published: December 20, 2006

References

- Abi-Gerges, N., Ji, G.J., Lu, Z.J., Fischmeister, R., Hescheler, J., and Fleischmann, B.K. (2000). Functional expression and regulation of the hyperpolarization activated non-selective cation current in embryonic stem cell-derived cardiomyocytes. *J. Physiol.* 523, 377–389.
- Balla, A., and Balla, T. (2006). Phosphatidylinositol 4-kinases: old enzymes with emerging functions. *Trends Cell Biol.* 16, 351–361.
- Baruscotti, M., Bucchi, A., and DiFrancesco, D. (2005). Physiology and pharmacology of the cardiac pacemaker (“funny”) current. *Pharmacol. Ther.* 107, 59–79.
- Baukrowitz, T., Schulte, U., Oliver, D., Herlitze, S., Krauter, T., Tucker, S.J., Ruppersberg, J.P., and Fakler, B. (1998). PIP₂ and PIP as determinants for ATP inhibition of KATP channels. *Science* 282, 1141–1144.
- Bildl, W., Strassmaier, T., Thurm, H., Andersen, J., Eble, S., Oliver, D., Knipper, M., Mann, M., Schulte, U., Adelman, J.P., and Fakler, B. (2004). Protein kinase CK2 is coassembled with small conductance Ca²⁺-activated K⁺ channels and regulates channel gating. *Neuron* 43, 847–858.
- Boyett, M.R., Honjo, H., and Kodama, I. (2000). The sinoatrial node, a heterogeneous pacemaker structure. *Cardiovasc. Res.* 47, 658–687.
- Brown, H.F., DiFrancesco, D., and Noble, S.J. (1979). How does adrenaline accelerate the heart? *Nature* 280, 235–236.

- Cerbai, E., Pino, R., Sartiani, L., and Mugelli, A. (1999). Influence of postnatal-development on I(f) occurrence and properties in neonatal rat ventricular myocytes. *Cardiovasc. Res.* 42, 416–423.
- Chen, S., Wang, J., and Siegelbaum, S.A. (2001). Properties of hyperpolarization-activated pacemaker current defined by coassembly of HCN1 and HCN2 subunits and basal modulation by cyclic nucleotide. *J. Gen. Physiol.* 117, 491–504.
- DiFrancesco, D. (1993). Pacemaker mechanisms in cardiac tissue. *Annu. Rev. Physiol.* 55, 455–472.
- DiFrancesco, D., and Mangoni, M. (1994). Modulation of single hyperpolarization-activated channels (i(f)) by cAMP in the rabbit sino-atrial node. *J. Physiol.* 474, 473–482.
- DiFrancesco, D., and Tortora, P. (1991). Direct activation of cardiac pacemaker channels by intracellular cyclic AMP. *Nature* 351, 145–147.
- DiFrancesco, D., Ferroni, A., Mazzanti, M., and Tromba, C. (1986). Properties of the hyperpolarizing-activated current (if) in cells isolated from the rabbit sino-atrial node. *J. Physiol.* 377, 61–88.
- Fakler, B., Brandle, U., Glowatzki, E., Weidemann, S., Zenner, H.P., and Ruppersberg, J.P. (1995). Strong voltage-dependent inward rectification of inward rectifier K⁺ channels is caused by intracellular spermine. *Cell* 80, 149–154.
- Fleischmann, B.K., Duan, Y., Fan, Y., Schoneberg, T., Ehlich, A., Lenka, N., Viatchenko-Karpinski, S., Pott, L., Hescheler, J., and Fakler, B. (2004). Differential subunit composition of the G protein-activated inward-rectifier potassium channel during cardiac development. *J. Clin. Invest.* 114, 994–1001.
- Frere, S.G., Kuisle, M., and Luthi, A. (2004). Regulation of recombinant and native hyperpolarization-activated cation channels. *Mol. Neurobiol.* 30, 279–305.
- Halliwel, J.V., and Adams, P.R. (1982). Voltage-clamp analysis of muscarinic excitation in hippocampal neurons. *Brain Res.* 250, 71–92.
- Huang, C.L., Feng, S., and Hilgemann, D.W. (1998). Direct activation of inward rectifier potassium channels by PIP₂ and its stabilization by Gbetagamma. *Nature* 391, 803–806.
- Kaupp, U.B., and Seifert, R. (2001). Molecular diversity of pacemaker ion channels. *Annu. Rev. Physiol.* 63, 235–257.
- Krauss, M., Kinuta, M., Wenk, M.R., De Camilli, P., Takei, K., and Haucke, V. (2003). ARF6 stimulates clathrin/AP-2 recruitment to synaptic membranes by activating phosphatidylinositol phosphate kinase type Igamma. *J. Cell Biol.* 162, 113–124.
- Ludwig, A., Zong, X., Jeglitsch, M., Hofmann, F., and Biel, M. (1998). A family of hyperpolarization-activated mammalian cation channels. *Nature* 393, 587–591.
- Ludwig, J., Oliver, D., Frank, G., Klocker, N., Gummer, A.W., and Fakler, B. (2001). Reciprocal electromechanical properties of rat prestin: the motor molecule from rat outer hair cells. *Proc. Natl. Acad. Sci. USA* 98, 4178–4183.
- Magee, J.C. (1999). Dendritic I_h normalizes temporal summation in hippocampal CA1 neurons. *Nat. Neurosci.* 2, 508–514.
- Milosevic, I., Sorensen, J.B., Lang, T., Krauss, M., Nagy, G., Haucke, V., Jahn, R., and Neher, E. (2005). Plasmalemmal phosphatidylinositol-4,5-bisphosphate level regulates the releasable vesicle pool size in chromaffin cells. *J. Neurosci.* 25, 2557–2565.
- Neuhoff, H., Neu, A., Liss, B., and Roeper, J. (2002). I(h) channels contribute to the different functional properties of identified dopaminergic subpopulations in the midbrain. *J. Neurosci.* 22, 1290–1302.
- Oliver, D., He, D.Z., Klocker, N., Ludwig, J., Schulte, U., Waldegger, S., Ruppersberg, J.P., Dallos, P., and Fakler, B. (2001). Intracellular anions as the voltage sensor of prestin, the outer hair cell motor protein. *Science* 292, 2340–2343.
- Oliver, D., Lien, C.C., Soom, M., Baukrowitz, T., Jonas, P., and Fakler, B. (2004). Functional conversion between A-type and delayed rectifier K⁺ channels by membrane lipids. *Science* 304, 265–270.
- Pape, H.C., and McCormick, D.A. (1989). Noradrenaline and serotonin selectively modulate thalamic burst firing by enhancing a hyperpolarization-activated cation current. *Nature* 340, 715–718.

- Pian, P., Bucchi, A., Robinson, R.B., and Siegelbaum, S.A. (2006). Regulation of gating and rundown of HCN hyperpolarization-activated channels by exogenous and endogenous PIP₂. *J. Gen. Physiol.* *128*, 593–604.
- Qu, J., Barbuti, A., Protas, L., Santoro, B., Cohen, I.S., and Robinson, R.B. (2001). HCN2 overexpression in newborn and adult ventricular myocytes: distinct effects on gating and excitability. *Circ. Res.* *89*, E8–E14.
- Robinson, R.B., and Siegelbaum, S.A. (2003). Hyperpolarization-activated cation currents: from molecules to physiological function. *Annu. Rev. Physiol.* *65*, 453–480.
- Robinson, R.B., Yu, H., Chang, F., and Cohen, I.S. (1997). Developmental change in the voltage-dependence of the pacemaker current, *if*, in rat ventricle cells. *Pflugers Arch.* *433*, 533–535.
- Rohacs, T., Lopes, C.M., Jin, T., Ramdya, P.P., Molnar, Z., and Logothetis, D.E. (2003). Specificity of activation by phosphoinositides determines lipid regulation of Kir channels. *Proc. Natl. Acad. Sci. USA* *100*, 745–750.
- Santoro, B., and Tibbs, G.R. (1999). The HCN gene family: molecular basis of the hyperpolarization-activated pacemaker channels. *Ann. N Y Acad. Sci.* *868*, 741–764.
- Santoro, B., Liu, D.T., Yao, H., Bartsch, D., Kandel, E.R., Siegelbaum, S.A., and Tibbs, G.R. (1998). Identification of a gene encoding a hyperpolarization-activated pacemaker channel of brain. *Cell* *93*, 717–729.
- Shyng, S.L., and Nichols, C.G. (1998). Membrane phospholipid control of nucleotide sensitivity of KATP channels. *Science* *282*, 1138–1141.
- Stevens, D.R., Seifert, R., Bufe, B., Muller, F., Kremmer, E., Gauss, R., Meyerhof, W., Kaupp, U.B., and Lindemann, B. (2001). Hyperpolarization-activated channels HCN1 and HCN4 mediate responses to sour stimuli. *Nature* *413*, 631–635.
- Ulens, C., and Siegelbaum, S.A. (2003). Regulation of hyperpolarization-activated HCN channels by cAMP through a gating switch in binding domain symmetry. *Neuron* *40*, 959–970.
- Vanhaesebroeck, B., Leever, S.J., Ahmadi, K., Timms, J., Katso, R., Driscoll, P.C., Woscholski, R., Parker, P.J., and Waterfield, M.D. (2001). Synthesis and function of 3-phosphorylated inositol lipids. *Annu. Rev. Biochem.* *70*, 535–602.
- Wainger, B.J., DeGennaro, M., Santoro, B., Siegelbaum, S.A., and Tibbs, G.R. (2001). Molecular mechanism of cAMP modulation of HCN pacemaker channels. *Nature* *411*, 805–810.
- Williams, S.R., and Stuart, G.J. (2000). Site independence of EPSP time course is mediated by dendritic I(h) in neocortical pyramidal neurons. *J. Neurophysiol.* *83*, 3177–3182.
- Woscholski, R., Waterfield, M.D., and Parker, P.J. (1995). Purification and biochemical characterization of a mammalian phosphatidylinositol 3,4,5-trisphosphate 5-phosphatase. *J. Biol. Chem.* *270*, 31001–31007.
- Zagotta, W.N., Olivier, N.B., Black, K.D., Young, E.C., Olson, R., and Gouaux, E. (2003). Structural basis for modulation and agonist specificity of HCN pacemaker channels. *Nature* *425*, 200–205.